Preprints of the 18th IFAC World Congress
Milano (Italy) August 28 - September 2, 2011

On the Optimization of Biogas Production in Anaerobic Digestion Systems ⋆

Mihaela Sbarciog * **Mia Loccufier** ** **Alain Vande Wouwer** *

* *UMONS, Automatic Control Laboratory, 31 Boulevard Dolez, 7000 Mons, Belgium (e-mail: {MihaelaIuliana.Sbarciog, Alain.Vandewouwer}@umons.ac.be)*
** *Ghent University, Electrical Energy, Systems and Automation, Technologiepark 914, 9052 Ghent, Belgium (e-mail: Mia.Loccufier@UGent.be)*

Abstract: This paper presents a strategy for the optimization of biogas outflow rate in an anaerobic digestion process described by a two-population model. The methodology relies on the solution of two optimization problems: steady state optimization for determining the optimal operating point and transient optimization. The latter is solved using the maximum principle of Pontryagin.
The proposed control law, which drives the process from an initial state to the optimal steady state while maximizing the biogas outflow rate, consists of switching the manipulated variable (dilution rate) from the minimum to the maximum value and then to the optimal value at well defined instants. This control law substantially increases the stability region of the optimal equilibrium point, enlarging it in some cases to almost the entire state space. Aside its efficiency, the strategy is also characterized by simplicity, being thus appropriate for implementation in real-life systems. Another important advantage is its generality: this technique may be applied to any anaerobic digestion process, for which the acidogenesis and methanogenesis are respectively characterized by Monod and Haldane kinetics.

Keywords: biotechnology, nonlinear systems, stability analysis, optimal control, bang-bang control

1. INTRODUCTION

Anaerobic digestion has gained considerable importance lately, being the most encountered process for the biological treatment of wastewater and biogas production. Compared to the aerobic treatment, the anaerobic digestion provides several advantages among which the higher energy production and the substantially lower sludge production are the most important ones. In terms of process stability, anaerobic digestion still lags behind aerobic biological treatment or physico-chemical processes. Substantial expertise is required to operate such a process properly. From a biological point of view, the main cause of the anaerobic digestion failure is the imbalance between the acid forming bacteria and the methane forming bacteria.

Many control strategies for anaerobic digestion processes have been proposed in the literature, which aim to either regulate the organic pollution level or to optimize the production of the methane gas. The most popular ones are robust output feedback control (Mailleret et al. (2003); Antonelli et al. (2003); Méndez-Acosta et al. (2010)) and adaptive control (Mailleret et al. (2004); Marcos et al. (2004); Dimitrova and Krastanov (2009)). Steyer et al. (2006) have reviewed a number of control strategies for anaerobic digestion systems and have concluded that neither the classical nor the advanced control methods have succeeded in overcoming all the difficulties which arise in the efficient operation of these processes.

More efficient and less complex control laws may be derived by exploiting the insight gained from a thorough analysis of system dynamics. This provides useful guidance for process operation and control (e.g. the methodology of detecting hazardous working modes developed by Hess and Bernard (2008, 2009)). This paper presents a methodology for the optimization of biogas production in anaerobic digestion systems. The control law is found by solving steady state and transient optimization problems and consists of switching the dilution rate from minimum to maximum and then to the optimal values at well determined time instants. The procedure is simplified by using one of the system stability boundaries as switching surface. In this way the optimal equilibrium state is reachable from almost the entire state space of the system. Aside its efficiency and simplicity, the method may be applied to any anaerobic digestion process, described by a two-population model, in which the acidogenesis and methanogenesis are respectively characterized by Monod and Haldane kinetics.

⋆ This paper presents research results of the Belgian Network DYSCO (Dynamical Systems, Control, and Optimization), funded by the Interuniversity Attraction Poles Programme, initiated by the Belgian State, Science Policy Office. The scientific responsibility rests with its author(s).

2. PROCESS DESCRIPTION

Throughout this paper, an anaerobic digestion model is considered, in which the biological transformations are given by the following reaction network:

$$\begin{aligned} a\xi_1 &\rightarrow c\xi_2 + \xi_3 \\ d\xi_2 &\rightarrow CH_4 + \xi_4 \end{aligned} \tag{1}$$

In the first reaction, the acidogenic bacteria ξ_3 grow on the organic substrate ξ_1 and produce volatile fatty acids ξ_2. In the second reaction, the methanogenic bacteria ξ_4 use the volatile fatty acids as substrate for growth and produce methane. When operating the anaerobic digestion process, a balance between the acidogenesis and methanogenesis must be maintained.

For an ideal continuous stirred tank reactor, the system dynamics described by the reaction network (1) are given by the following differential equations:

$$\dot{\xi}_1 = u(\xi_{in_1} - \xi_1) - a r_1(\xi) \tag{2}$$
$$\dot{\xi}_2 = u(\xi_{in_2} - \xi_2) + c r_1(\xi) - d r_2(\xi) \tag{3}$$
$$\dot{\xi}_3 = -u\xi_3 + r_1(\xi) \tag{4}$$
$$\dot{\xi}_4 = -u\xi_4 + r_2(\xi) \tag{5}$$

while the outflow rate of methane gas reads:

$$Q(\xi) = q\mu_2(\xi_2)\xi_4 \tag{6}$$

In equations (2)-(6), u represents the dilution rate and ξ_{in_1}, ξ_{in_2} respectively represent the concentrations of organic substrate and of volatile fatty acids in the influent. $a, c, d > 0$ are the stoichiometric coefficients. $q > 0$ is the yield for the methane production. $\xi = [\,\xi_1 \;\; \xi_2 \;\; \xi_3 \;\; \xi_4\,]' \in \mathbb{R}^{+^4}$ denotes the state vector. The reaction rates $r_1(\xi)$, $r_2(\xi)$ read:

$$r_1(\xi) = \mu_1(\xi_1)\xi_3 \quad r_2(\xi) = \mu_2(\xi_2)\xi_4 \tag{7}$$

where the growth functions are respectively of Monod and Haldane type

$$\mu_1(\xi_1) = \mu_{m_1}\frac{\xi_1}{K_{s_1} + \xi_1} \tag{8}$$

$$\mu_2(\xi_2) = \mu_{m_2}\frac{\xi_2}{K_{s_2} + \xi_2 + \frac{\xi_2^2}{K_{i_2}}} \tag{9}$$

Table 1 gives the numerical values/ranges for the anaerobic digestion model parameters and input variables, used for the simulation results.

Table 1. Numerical values/ranges of the anaerobic digestion model parameters and input variables (as in Bernard et al. (2001))

a	42.14		K_{s_1}	7.1	g/l
c	116.5	mmole/g	K_{s_2}	9.28	mmole/l
d	268	mmole/g	K_{i_2}	256	mmole/l
q	453	mmole/g	ξ_{in_1}	$[\,0 \;\; 50\,]$	g/l
μ_{m_1}	1.2	day^{-1}	ξ_{in_2}	$[\,0 \;\; 200\,]$	mmole/l
μ_{m_2}	0.74	day^{-1}	u	$[\,0 \;\; 1.5\,]$	day^{-1}

By considering a partition of the state vector of the form $\xi = [\,\xi_a \;\; \xi_b\,]'$, where $\xi_a = [\,\xi_3 \;\; \xi_4\,]'$ and $\xi_b = [\,\xi_1 \;\; \xi_2\,]'$, and a linear transformation of the states $x_a = \xi_a$, $x_b = \xi_b - C_b C_a^{-1}\xi_a$, a canonical state space representation of the anaerobic digestion system can be obtained (Bastin and Dochain (1990)):

$$\dot{x}_a = u(w_a - x_a) + C_a\rho(x) \tag{10}$$
$$\dot{x}_b = u(w_b - x_b) \tag{11}$$

with

$$x_a \triangleq \begin{bmatrix} x_3 \\ x_4 \end{bmatrix} \in \mathbb{R}^{+^2};\; x_b \triangleq \begin{bmatrix} x_1 \\ x_2 \end{bmatrix} \in \mathbb{R}^2;$$
$$C_a = I_2;\; C_b = \begin{bmatrix} -a & 0 \\ c & -d \end{bmatrix};$$
$$\rho(x) \triangleq \begin{bmatrix} \rho_1(x) \\ \rho_2(x) \end{bmatrix} \in \mathbb{R}^{+^2};$$
$$\rho_i(x) = r_i(\xi)|_{\xi_a = x_a;\; \xi_b = x_b + C_b C_a^{-1} x_a},\; i = 1, 2$$
$$w_a = \begin{bmatrix} w_3 \\ w_4 \end{bmatrix} \triangleq \begin{bmatrix} 0 \\ 0 \end{bmatrix};\; w_b = \begin{bmatrix} w_1 \\ w_2 \end{bmatrix} \triangleq \begin{bmatrix} \xi_{in_1} \\ \xi_{in_2} \end{bmatrix} \in \mathbb{R}^{+^2}$$

The canonical model consists of a nonlinear part of dimension 2 dynamically coupled with a linear part of dimension 2. To preserve the positiveness property of the original system, physical boundary conditions are imposed, which define the state space of the canonical model as:

$$S_x = \big\{x \in \mathbb{R}^4;\; \xi_1 = x_1 - a x_3 \geq 0;\; \xi_2 = x_2 + c x_3 - d x_4 \geq 0$$
$$\xi_3 = x_3 \geq 0;\; \xi_4 = x_4 \geq 0\big\}$$

A detailed analysis of this model has been performed by Sbarciog et al. (2010a). For the development of the control strategy, the main properties of the system are summarized here. The anaerobic digestion system (10), (11) has bounded solutions and is a non-oscillatory system. This means that the set of equilibria is globally convergent: as time increases every system solution converges to an equilibrium point. The equilibria are the solutions of

$$x_1 = w_1 = \xi_{in_1} \tag{12}$$
$$x_2 = w_2 = \xi_{in_2} \tag{13}$$
$$[-u + \mu_1(\xi_1)]\, x_3 = 0 \tag{14}$$
$$[-u + \mu_2(\xi_2)]\, x_4 = 0 \tag{15}$$

All equilibria lie on the plane

$$\Delta = \{x \in S_x;\; x_1 = w_1,\; x_2 = w_2\}$$

The number of physical equilibrium points and their stability properties depend on the magnitude of dilution rate u and of concentrations in the influent of organic substrate ξ_{in_1} and volatile fatty acids ξ_{in_2}.

The equilibrium equations (14), (15) lead to several possibilities:

(i) $x_3 = 0$ and $x_4 = 0$
This defines the equilibrium point A.

(ii) $x_4 = 0$ and $\mu_1(\xi_1) = u$
This defines the equilibrium point B, where $\hat{\xi}_{1,B}$ is the unique solution of

$$\mu_1(\xi_1) = u \tag{18}$$

(iii) $x_3 = 0$ and $\mu_2(\xi_2) = u$
This defines the equilibria C and D, generically denoted by M, where $\hat{\xi}_{2,C}$ and $\hat{\xi}_{2,D}$ (with $\hat{\xi}_{2,C} < \hat{\xi}_{2,D}$) are the two solutions of

$$\mu_2(\xi_2) = u \tag{19}$$

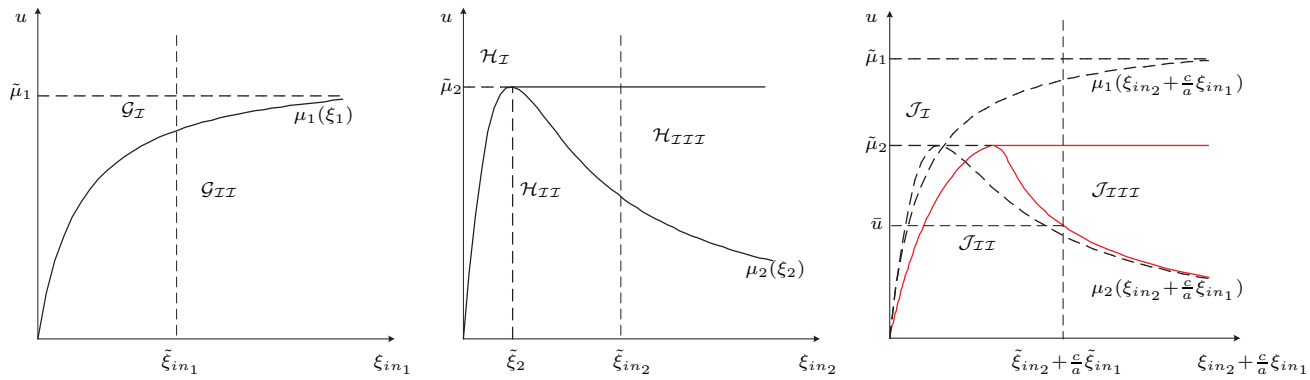

Fig. 1. Relationship between the dilution rate u and concentrations of components in the influent ξ_{in_1}, ξ_{in_2} determining a different number of equilibrium points: the regions are bounded by continuous lines

Table 2. The analytical expressions of the system equilibria

Canonical states	Physical states
$\hat{x}_A = \begin{bmatrix} w_1 \\ w_2 \\ 0 \\ 0 \end{bmatrix}$	$\hat{\xi}_A = \begin{bmatrix} \xi_{in_1} \\ \xi_{in_2} \\ 0 \\ 0 \end{bmatrix}$
$\hat{x}_B = \begin{bmatrix} w_1 \\ w_2 \\ \frac{1}{a}(w_1 - \hat{\xi}_{1,B}) \\ 0 \end{bmatrix}$	$\hat{\xi}_B = \begin{bmatrix} \hat{\xi}_{1,B} \\ \xi_{in_2} + \frac{c}{a}(\xi_{in_1} - \hat{\xi}_{1,B}) \\ \frac{1}{a}(\xi_{in_1} - \hat{\xi}_{1,B}) \\ 0 \end{bmatrix}$
$\hat{x}_M = \begin{bmatrix} w_1 \\ w_2 \\ 0 \\ \frac{1}{d}(w_2 - \hat{\xi}_{2,M}) \end{bmatrix}$	$\hat{\xi}_M = \begin{bmatrix} \xi_{in_1} \\ \hat{\xi}_{2,M} \\ 0 \\ \frac{1}{d}(\xi_{in_2} - \hat{\xi}_{2,M}) \end{bmatrix}$; $M = C, D$
$\hat{x}_N = \begin{bmatrix} w_1 \\ w_2 \\ \frac{1}{a}(w_1 - \hat{\xi}_{1,N}) \\ \hat{x}_{4,N} \end{bmatrix}$	$\hat{\xi}_N = \begin{bmatrix} \hat{\xi}_{1,N} \\ \hat{\xi}_{2,N} \\ \frac{1}{a}(\xi_{in_1} - \hat{\xi}_{1,N}) \\ \hat{\xi}_{4,N} \end{bmatrix}$; $N = E, F$

$$\hat{x}_{4,N} = \frac{1}{d}\left[w_2 - \hat{\xi}_{2,N} + \frac{c}{a}(w_1 - \hat{\xi}_{1,N})\right] \quad (16)$$

$$\hat{\xi}_{4,N} = \frac{1}{d}\left[\xi_{in_2} - \hat{\xi}_{2,N} + \frac{c}{a}(\xi_{in_1} - \hat{\xi}_{1,N})\right] \quad (17)$$

(iv) $\mu_1(\xi_1) = u$ and $\mu_2(\xi_2) = u$
This defines the equilibria E and F, generically denoted by N, where $\hat{\xi}_{1,E} = \hat{\xi}_{1,F}$ is the solution of (18) and $\hat{\xi}_{2,E}$ and $\hat{\xi}_{2,F}$ (with $\hat{\xi}_{2,E} < \hat{\xi}_{2,F}$) are the solutions of (19).

Table 2 presents the analytical expressions of the equilibrium points in the canonical states respectively in the physical states, while Fig. 1 presents regions in the spaces $(\xi_{in_1}; u)$, $(\xi_{in_2}; u)$ and $\left(\xi_{in_2} + \frac{c}{a}\xi_{in_1}; u\right)$ corresponding to the occurrence of physical equilibrium points. The total wash out of the system $\hat{x}_A$ $(\hat{\xi}_A)$ is always a physical equilibrium point. $\hat{x}_B$ $(\hat{\xi}_B)$, characterized by the wash out of methanogenic bacteria, is physical if $(\xi_{in_1}, u) \in \mathcal{G}_{\mathcal{II}}$. The two equilibria $\hat{x}_M$ $(\hat{\xi}_M)$, characterized by acidogenic bacteria wash out, are respectively physical if $(\xi_{in_2}, u) \in \mathcal{H}_{\mathcal{II}} \cup \mathcal{H}_{\mathcal{III}}$ for $M = C$ and $(\xi_{in_2}, u) \in \mathcal{H}_{\mathcal{III}}$ for $M = D$. The two equilibria $\hat{x}_N$ $(\hat{\xi}_N)$, characterized by the presence of both bacteria type, are physical if $(\xi_{in_1}, u) \in \mathcal{G}_{\mathcal{II}}$ and respectively $\left(\xi_{in_2} + \frac{c}{a}\xi_{in_1}, u\right) \in \mathcal{J}_{\mathcal{II}} \cup \mathcal{J}_{\mathcal{III}}$ for $N = E$ and $\left(\xi_{in_2} + \frac{c}{a}\xi_{in_1}, u\right) \in \mathcal{J}_{\mathcal{III}}$ for $N = F$. The stability of equilibria has been assessed via the linearization principle (see Sbarciog et al. (2010a)). The following characteristics are useful for the further development of the control strategy:

- $\hat{x}_E$ is always locally asymptotically stable;
- $\hat{x}_F$ is always unstable;
- $\hat{x}_B$ is locally asymptotically stable in the region where $\hat{x}_F$ is physical (i.e. $\mathcal{J}_{\mathcal{III}}$) and unstable in the region where $\hat{x}_F$ is not physical (i.e. $\mathcal{J}_{\mathcal{II}}$).

Usually in practice only the dilution rate u can be manipulated, therefore in what follows the inlet concentrations ξ_{in_1} and ξ_{in_2} are considered fixed and set respectively to the values $\tilde{\xi}_{in_1} = 40$ g/l and $\tilde{\xi}_{in_2} = 175$ mmol/l for the simulation results.

3. OPTIMIZATION

The control purpose is to optimize the outflow rate of methane (6) by manipulating the dilution rate u, with $u \in [u_{min}, u_{max}]$. The numerical values of u_{min} and u_{max} are selected based on a number of considerations discussed in the next section. During the transient an optimal production of biogas is pursued, possibly taking into account some costs (e.g. minimize the work of the actuator). At the end of the transient period the process should reach a steady state in which the outflow rate of biogas is maximum. Hence the control strategy proposed in this section performs transient as well as steady state optimization.

3.1 Steady state optimization

The steady state optimization problem is defined as follows: *Find the optimal setpoint $\hat{x}_s$ $(\hat{\xi}_s)$ and the corresponding optimal dilution rate u_s for which the outflow rate of methane $Q(\hat{\xi}_s)$ is maximum.*

The analysis summarized in the previous section shows that the only technologically meaningful equilibrium points are $\hat{x}_E$ and $\hat{x}_F$. Both are characterized by methane production. It is easy to see however, that the flow rate of methane produced in $\hat{\xi}_E$ is higher than the flow rate of methane produced in $\hat{\xi}_F$ ($\mu_2(\hat{\xi}_{2,E}) = \mu_2(\hat{\xi}_{2,F}) = u$ and according to (17), $\hat{\xi}_{4,E} > \hat{\xi}_{4,F}$ because $\hat{\xi}_{2,E} = \hat{\xi}_{2,C} < \hat{\xi}_{2,F} = \hat{\xi}_{2,D}$). Consequently, the optimal setpoint is an equilibrium

point of type E. Thus, in the optimal equilibrium point $\hat{\xi}_s$ the flow rate of methane is given by

$$Q(\hat{\xi}_s) = q\mu_2(\hat{\xi}_{2,s})\frac{1}{d}\left[\xi_{in_2} - \hat{\xi}_{2,s} + \frac{c}{a}(\xi_{in_1} - \hat{\xi}_{1,s})\right] \quad (20)$$

Calculating $\left.\frac{dQ}{d\xi_2}\right|_{\xi_2=\hat{\xi}_{2,s}} = 0$ leads to

$$\left[\xi_{in_2} - \hat{\xi}_{2,s} + \frac{c}{a}(\xi_{in_1} - \hat{\xi}_{1,s})\right] \cdot \mu_{2_d}(\hat{\xi}_{2,s}) - \mu_2(\hat{\xi}_{2,s})\left(1 + \frac{c}{a}\left.\frac{d\xi_1}{d\xi_2}\right|_{\xi_2=\hat{\xi}_{2,s}}\right) = 0 \quad (21)$$

where $\left.\frac{d\xi_1}{d\xi_2}\right|_{\xi_2=\hat{\xi}_{2,s}}$ results from

$$\mu_{1_d}(\hat{\xi}_{1,s})\left.\frac{d\xi_1}{d\xi_2}\right|_{\xi_2=\hat{\xi}_{2,s}} = \mu_{2_d}(\hat{\xi}_{2,s}) \quad (22)$$

with μ_{2_d} denoting the derivative of μ_2 w.r.t. ξ_2 and μ_{1_d} denoting the derivative of μ_1 w.r.t. ξ_1.

Recall that the optimal setpoint is a type E equilibrium point where

$$\mu_1(\hat{\xi}_{1,s}) = \mu_2(\hat{\xi}_{2,s}) = u_s \quad (23)$$

Then (21) and (23) provide sufficient conditions to fully determine the optimal equilibrium point $\hat{\xi}_s$ and the optimal dilution rate u_s.

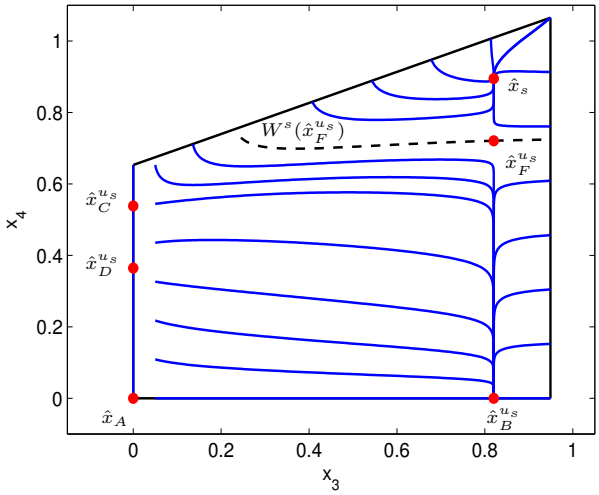

Fig. 2. The phase portrait on the Δ plane of the system operated with the dilution rate u_s

Fig. 2 presents the phase portrait on the Δ plane of the system operated with the optimal dilution rate u_s (the superscript in the notation of equilibria indicates the dilution rate). The optimal setpoint $\hat{x}_s$ may be reached only if the initial state of the system lies above the stability boundary $W^s(\hat{x}_F^{u_s})$ (represented with a dashed line), which delimits the region of attractions of the optimal setpoint $\hat{x}_s$ ($\Omega(\hat{x}_s)$) and of the acidification point $\hat{x}_B^{u_s}$ ($\Omega(\hat{x}_B^{u_s})$).

3.2 Transient optimization

The transient optimization problem is formulated as a free final time optimal control problem of the form: *Find the dilution rate* $u(t) \in [u_{min}, u_{max}]$ *which drives, in finite time, the system* (10), (11) *from an initial state at time* $t = 0$ *to a small neighbourhood* S *of the steady state optimal equilibrium point* $\hat{x}_s$*, while minimizing a cost index of the form*

$$J(D) = \int_0^{t_f} [\alpha_1 u - Q]\, dt = \int_0^{t_f} [\alpha_1 u - q\mu_2(\xi_2)\xi_4]\, dt \quad (24)$$

where t_f represents the final time of the control interval and α_1 is a weighting coefficient. As soon as the system state reaches the neighbourhood S (target set) the control effort is switched to $u = u_s$, which ensures the convergence to the optimal steady state for $t \to +\infty$. The target set is generically defined as

$$S = \{x \in S_x;\ \theta(x) = 0\} \quad (25)$$

where $\theta(x)$ is a function of system states. Indications regarding its choice are given below.

The transient optimization is a classical optimal control problem, which can be solved using Pontryagin's maximum principle. Consequently, minimizing the cost index (24) is equivalent to maximizing the Hamiltonian, which is linear in the control input

$$\mathcal{H} = \underbrace{\left[\alpha_1 + \sum_{i=1}^{4} p_i(w_i - x_i)\right]}_{s_1(x,p)} u + \underbrace{p_3\mu_1(\xi_1)x_3 + (p_4 - q)\mu_2(\xi_2)x_4}_{s_2(x,p)} \quad (26)$$

$p = [\,p_1\ p_2\ p_3\ p_4\,]'$ is the costate vector, where

$$\dot{p}_i = -\frac{\partial \mathcal{H}}{\partial x_i}, \quad i = 1 \ldots 4 \quad (27)$$

and the transversality conditions are

$$\left[\left(\frac{\partial \theta}{\partial x}\right)' \lambda - p\right]_{t=t_f} = 0 \quad (28)$$

where λ denotes the Lagrange multipliers.

Hence by the maximum principle, if in an interval (t_1, t_2):

$$s_1(x,p) > 0 \Rightarrow u(t) = u_{min} \quad \text{for} \quad t_1 < t < t_2 \quad (29)$$

$$s_1(x,p) < 0 \Rightarrow u(t) = u_{max} \quad \text{for} \quad t_1 < t < t_2 \quad (30)$$

$$s_1(x,p) = 0 \Rightarrow (t_1, t_2) \ \text{is a singular interval} \quad (31)$$

Similarly to Sbarciog et al. (2008), it can be shown that singular intervals cannot occur, because $\dot{s}_1(x,p) < 0$. Hence it may be concluded that:

- the optimal control strategy is of the bang-bang type with at most one switching, from u_{min} to u_{max};
- in the state space of system (10), (11) there exists a switching surface $s_1(x) = 0$ such that for $x \notin S$:

$$s_1(x) > 0 \Rightarrow u = u_{min}$$

$$s_1(x) < 0 \Rightarrow u = u_{max}$$

- for $x \in S$, $u = u_s$.

The switching surface $s_1(x) = 0$ depends on the choice of the target set S and on the weighting parameter α_1 in the cost index. Its determination requires the solution of a set of nonlinear canonical differential equations (10), (11), (27)

with split boundary conditions (initial conditions at $t = 0$, final conditions and transversality conditions at $t = t_f$), which generally constitute a difficult numerical problem (see Banga et al. (2005) and references therein). In order to avoid this issue the switching is chosen to take place on a heuristically selected switching surface.

Selecting an appropriate target set and switching surface by trial-and-error may be a time consuming task, due to the numerous conditions the switching surface must satisfy. These conditions have to be checked by simulation. Sbarciog et al. (2008) suggested to switch the dilution rate from the minimum to the maximum allowable values once the system trajectory reaches the stability boundary of the system nominal operating point corresponding to the maximum dilution rate, that is $\partial\Omega(\hat{x}_E^{u_{max}}) = W^s(\hat{x}_F^{u_{max}})$.

A detailed description of estimating the stability boundary for the anaerobic digestion model (10), (11) can be found in Sbarciog et al. (2010b). A simple choice for the target set is an ellipsoid or ball with the center at the optimal setpoint $\hat{x}_s$ and radius such that $\hat{x}_E^{u_{max}}$ lies inside the target set.

4. DISCUSSION AND SIMULATION RESULTS

The control strategy described in the previous section indicates that the system must be operated with the dilution rate u_{min} until the switching surface $W^s(\hat{x}_F^{u_{max}})$ is reached. Then, $u = u_{max}$ and the system is operated with the new dilution rate until it enters the target set S. Once inside the target set, the dilution rate is switched to the optimal dilution rate u_s and the system will settle down in the optimal equilibrium point $\hat{x}_s$.

For the parameter values given in Table 1 and $\xi_{in_1} = \tilde{\xi}_{in_1}$, $\xi_{in_2} = \tilde{\xi}_{in_2}$, steady state optimization leads to the optimal dilution rate $u_s = 0.5179$ day^{-1} and the corresponding optimal equilibrium point

$$\hat{x}_s = [\,40\ \ 175\ \ 0.82\ \ 0.9\ \,]'$$
$$\hat{\xi}_s = [\,5.39\ \ 29.65\ \ 0.82\ \ 0.9\ \,]'$$

This means that $(\xi_{in_1}, u_s) \in \mathcal{G}_{\mathcal{III}}$, $(\xi_{in_2}, u_s) \in \mathcal{H}_{\mathcal{III}}$, $\left(\xi_{in_2} + \frac{c}{a}\xi_{in_1}, u_s\right) \in \mathcal{J}_{\mathcal{III}}$, case in which all six equilibria are physical.

$$\theta(x_3, x_4) = (x_3 - x_{3,s})^2 / r_x^2 + (x_4 - x_{4,s})^2 / r_y^2 - 1 = 0$$

is the target set, with $r_x = 0.015$, $r_y = 0.07$.

While u_s is the solution of the steady state optimization problem, the minimum and maximum dilution rates u_{min} and u_{max} must be selected according to the system characteristics and technological considerations. Below, the selection of u_{min} and u_{max} based on the system characteristics is presented, technological considerations will be detailed elsewhere. Consequently, the maximum dilution rate $u_{max} > u_s$ must be chosen such that $\hat{x}_E^{u_{max}}$ and $\hat{x}_F^{u_{max}}$ are physical equilibrium points, which means that $u_{max} < \tilde{\mu}_2$ (see Fig. 1). Values of u_{max} higher than $\tilde{\mu}_2 = \frac{\mu_{m_2}}{1+2\sqrt{\frac{K_{s_2}}{K_{i_2}}}}$ correspond to situations in which there is no production of biogas. Here, $u_{max} = 0.535$ day^{-1} ($\tilde{\mu}_2 = 0.536$) and the same situation as for u_s, characterized by the maximum number of physical equilibrium points, is obtained.

With regard to the minimum dilution rate $u_{min} < u_s$, two alternatives may be possible: $u_{min} \geq \bar{u}$ and $u_{min} < \bar{u}$ (see Fig. 1). $\bar{u}$ is the dilution rate for which $\hat{\xi}_{2,N} + \frac{c}{a}\hat{\xi}_{1,N} = \tilde{\xi}_{in_2} + \frac{c}{a}\tilde{\xi}_{in_1}$ and can be computed from (18) and (19). For the parameter values given in Table 1, $\bar{u} = 0.3495$ day^{-1}. Simulation results are presented below for both situations:

(1) $u_{min} \geq \bar{u}$

This case corresponds to $(\xi_{in_1}, u_{min}) \in \mathcal{G}_{\mathcal{III}}$, $(\xi_{in_2}, u_{min}) \in \mathcal{H}_{\mathcal{III}}$, $\left(\xi_{in_2} + \frac{c}{a}\xi_{in_1}, u_{min}\right) \in \mathcal{J}_{\mathcal{III}}$ (see Fig. 1), hence both $\hat{x}_E^{u_{min}}$ and $\hat{x}_F^{u_{min}}$ are physical equilibrium points. Thus the number of equilibria of the controlled system does not change with switching the dilution rate. Fig. 3 shows the phase portrait on the Δ plane of the controlled system. The minimum dilution rate has been chosen as $u_{min} = 0.38$ day^{-1}. Triangles, squares and circle respectively represent the equilibria corresponding to u_{min}, u_{max} and u_s. Dashed lines represent the system stability boundaries $W^s(\hat{x}_F^{u_{min}})$ and $W^s(\hat{x}_F^{u_{max}})$. It is worth to notice the enlargement of the attraction region of the optimal equilibrium point compared to the one shown in Fig. 2: now $\Omega(\hat{x}_s)$ equals the attraction region of $\hat{x}_E^{u_{min}}$. Hence, any system trajectory starting in an initial state lying above $W^s(\hat{x}_F^{u_{min}})$ reaches the optimal setpoint $\hat{x}_s$.

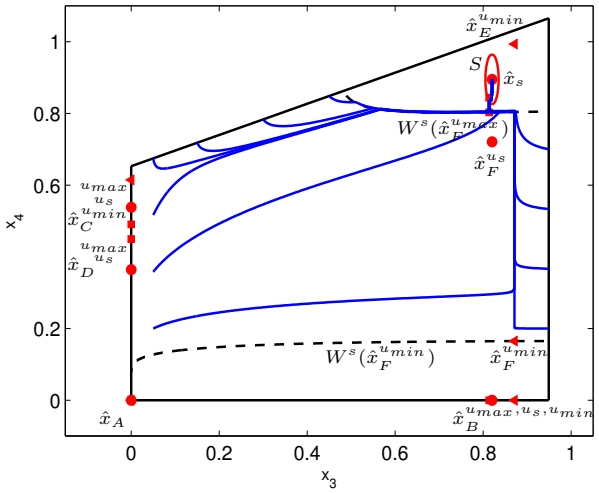

Fig. 3. The phase portrait on the Δ plane of the controlled system (case 1)

(2) $u_{min} < \bar{u}$

This case corresponds to $(\xi_{in_1}, u_{min}) \in \mathcal{G}_{\mathcal{II}}$, $(\xi_{in_2}, u_{min}) \in \mathcal{H}_{\mathcal{II}}$, $\left(\xi_{in_2} + \frac{c}{a}\xi_{in_1}, u_{min}\right) \in \mathcal{J}_{\mathcal{II}}$, where the system possesses four physical equilibria: $\hat{x}_A^{u_{min}}$, $\hat{x}_B^{u_{min}}$, $\hat{x}_C^{u_{min}}$, $\hat{x}_E^{u_{min}}$. Only $\hat{x}_E^{u_{min}}$ is locally asymptotically stable: every trajectory starting in an initial state characterized by the presence in the reactor of both bacteria type ($x_3 > 0$, $x_4 > 0$) will converge to it.

A question that may be raised in this case is whether or not the change in the structure of the phase portrait imposes additional constraints on the magnitude of u_{min}. As in the previous case, in order to be able to switch the dilution rate when the system trajectory hits the stability boundary $W^s(\hat{x}_F^{u_{max}})$, $\hat{x}_E^{u_{min}}$ must lie in $\Omega(\hat{x}_E^{u_{max}})$. Otherwise, the system

settles down in $\hat{x}_E^{u_{min}}$ and the optimal setpoint will not be reached. It may be checked however, that irrespective of the choice of u_{min}, this will not be the case: since all equilibria lie on the plane Δ, it is easy to show (based on the analytical expressions of the equilibria from Table 2) that $\hat{x}_E^{u_{min}}$ lies above $W^s(\hat{x}_F^{u_{max}})$.

Fig. 4 shows the phase portrait on the Δ plane of the controlled system. The minimum dilution rate has been chosen as $u_{min} = 0.3$ day^{-1}. The optimal equilibrium point $\hat{x}_s$ can be reached now from any initial state characterized by the presence in the reactor of both bacteria type. Hence $\hat{x}_s$ is quasi-globally asymptotically stable.

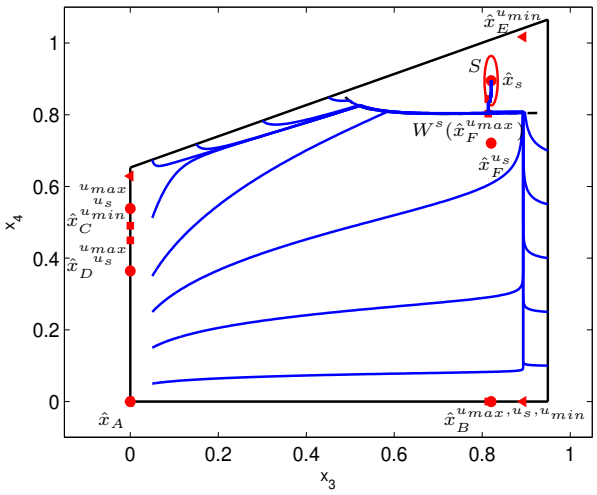

Fig. 4. The phase portrait on the Δ plane of the controlled system (case 2)

5. CONCLUSION

In this paper a control strategy for optimizing the biogas production in anaerobic digestion systems has been presented. The procedure consists of steady state optimization as well as transient optimization. A simple control law has been derived: the system must be operated with the minimum dilution rate u_{min} until the switching surface is reached, then it must be operated with the maximum dilution rate u_{max} until it enters a small neighbourhood of the optimal equilibrium point where the dilution rate is changed to u_s. The proposed control strategy enlarges considerably the region of attraction of the optimal equilibrium point, which for some values of the minimum dilution rate u_{min} becomes quasi-globally asymptotically stable.

To avoid the tremendous simulation work required for the selection of an appropriate switching surface, one of the system stability boundaries is used to switch the dilution rate from u_{min} to u_{max}. This boundary can be accurately estimated using algorithms that involve a low computational effort.

The proposed technique may be applied to any anaerobic digestion system, taking place in a bioreactor operated in continuous mode and described by a two-population model, in which the acidogenesis and methanogenesis are respectively characterized by Monod and Haldane kinetics.

ACKNOWLEDGEMENTS

M. Sbarciog thanks Prof. E.I.P. Volcke from Ghent University, Belgium, for suggesting this interesting process.

REFERENCES

Antonelli, R., Harmand, J., Steyer, J.P., and Astolfi, A. (2003). Set-point regulation of an anaerobic digestion process with bounded output feedback. *IEEE Trans. on Control Systems Technology*, 11, 495–504.

Banga, J.R., Balsa-Canto, E., Moles, C.G., and Alonso, A.A. (2005). Dynamic optimization of bioprocesses: Efficient and robust numerical strategies. *Journal of Biotechnology*, 117, 407–419.

Bastin, G. and Dochain, D. (1990). *On-line Estimation and Adaptive Control of Bioreactors*. Elsevier, Amsterdam.

Bernard, O., Hadj-Sadok, Z., Dochain, D., Genovesi, A., and Steyer, J.P. (2001). Dynamical model development and parameter identification for an anaerobic wastewater treatment process. *Biotechnology and Bioengineering*, 75, 424–438.

Dimitrova, N. and Krastanov, M. (2009). Nonlinear stabilizing control of an uncertain bioprocess model. *International Journal of Applied Mathematics and Computer Science*, 19, 441–454.

Hess, J. and Bernard, O. (2008). Design and study of a risk management criterion for an unstable anaerobic wastewater treatment process. *Journal of Process Control*, 18, 71–79.

Hess, J. and Bernard, O. (2009). Advanced dynamical risk analysis for monitoring anaerobic digestion process. *Biotechnology Progress*, 25, 643–653.

Mailleret, L., Bernard, O., and Steyer, J.P. (2003). Robust regulation of anaerobic digestion processes. *Water Science & Technology*, 48, 87–94.

Mailleret, L., Bernard, O., and Steyer, J.P. (2004). Nonlinear adaptive control for bioreactors with unknown kinetics. *Automatica*, 40, 1379–1385.

Marcos, N.I., Guay, M., Dochain, D., and Zhang, T. (2004). Adaptive extremum-seeking control of a continuous stirred tank bioreactor with haldane's kinetics. *Journal of Process Control*, 14, 317–328.

Méndez-Acosta, H.O., Palacios-Ruiz, B., Alcaraz-González, V., González-Álvarez, V., and García-Sandoval, J.P. (2010). A robust control scheme to improve the stability of anaerobic digestion processes. *Journal of Process Control*, 20, 375–383.

Sbarciog, M., Loccufier, M., and Noldus, E. (2008). Optimality and stability in a class of bang-bang controlled biochemical reaction systems. *International Journal of Control*, 81, 836–850.

Sbarciog, M., Loccufier, M., and Noldus, E. (2010a). Determination of appropriate operating strategies for anaerobic digestion systems. *Biochemical Engineering Journal*, 51, 180–188.

Sbarciog, M., Loccufier, M., and Noldus, E. (2010b). The estimation of stability boundaries for an anaerobic digestion system. In *Proceedings of the 11th International Symposium on Computer Applications in Biotechnology*, 359–364. Leuven, Belgium.

Steyer, J.P., Bernard, O., Batstone, D., and Angelidaki, I. (2006). Lessons learnt from 15 years of ica in anaerobic digesters. *Water Science & Technology*, 53, 25–33.